

CALIBRATION OF A FUEL RELOCATION MODEL IN BISON

Laura P. Swiler

Optimization and Uncertainty Quantification Dept.
Sandia National Laboratories
Albuquerque, NM 87185-1318
lpswile@sandia.gov

Richard L. Williamson and Danielle M. Perez

Fuels Modeling and Simulation Dept.
Idaho National Laboratory
Idaho Falls, ID 83415
richard.williamson@inl.gov; danielle.perez@inl.gov

ABSTRACT

We demonstrate parameter calibration in the context of the BISON nuclear fuels performance analysis code. Specifically, we present the calibration of a parameter governing fuel relocation: the power level at which the relocation model is activated. This relocation activation parameter is a critical value in obtaining reasonable comparison with fuel centerline temperature measurements. It also is the subject of some debate in terms of the optimal values. We show that the optimal value does vary across the calibration to individual rods. We also demonstrate an aggregated calibration, where we calibrate to observations from six rods.

Key Words: calibration, parameter estimation, relocation models

1. INTRODUCTION

Sensitivity analysis, uncertainty quantification, and calibration (e.g. parameter estimation) are typically performed after a model has been completely developed in an analysis stage. Using these tools can be useful during the model development stage as well. In the model development stage, sensitivity analysis and uncertainty quantification can inform developers about the behavior of various parameterizations and also help as a debugging tool. Calibration may be used to understand optimal values of parameters that yield good comparisons with existing data sets, and also to understand how one model may differ from another with respect to certain parameters.

In this paper, we demonstrate the use of parameter calibration in the context of BISON, which is an implicit, parallel, fully-coupled nuclear fuel performance code under development at Idaho National Laboratory [1]. BISON is built on the MOOSE computational framework [2] which allows for rapid development of codes involving the solution of partial differential equations using the finite element method. Nuclear fuel operates in an environment with complex multiphysics phenomena, occurring over distances ranging from inter-atomic spacing to meters, and times scales ranging from microseconds to years. This multiphysics behavior is often tightly coupled and many important aspects are inherently multidimensional. Most current fuel modeling codes employ loose multiphysics coupling and are restricted to 2D axisymmetric or 1.5D approximations [4–6]. BISON is able to simulate tightly coupled multiphysics and multiscale fuel behavior, for either 2D axisymmetric or 3D geometries. Although the primary development focus thus far has been on simulating light water reactor fuel rods, BISON has also been

applied to TRISO particle fuel in high temperature gas reactors and metallic fuel in both rod or plate form [1, 7]. BISON code validation and assessment is presented in [3].

We present the calibration of a parameter governing fuel relocation in BISON. Fuel performance codes have traditionally employed highly empirical relocation models to account for fuel cracking, which is known to occur, but is not captured mechanistically. For the relocation model implemented in BISON, there is a parameter which controls the power level at which the relocation model is activated. This relocation activation parameter is a critical value in obtaining reasonable comparison with fuel centerline temperature measurements. It also is the subject of some debate in terms of the optimal values. For this reason, we focused the calibration exercise on determining the optimal value of the power level at which the relocation model is activated. We will refer to this value as the relocation activation parameter.

The outline of the paper is as follows: We present calibration algorithms and the DAKOTA software framework we are using for optimization in Section 2. In Section 3, we present the Halden experimental dataset and outline the particular problem of interest. Section 4 provides the results, and Section 5 has some summary comments and next steps.

2. CALIBRATION

Calibration of model parameters involves a problem formulation which is solved with optimization algorithms. Calibration is often referred to by different names, depending on the terminology of the particular discipline: parameter estimation, system identification, parameter tuning, or inverse problems. In this paper, we use calibration to mean the estimation of “optimal” parameter values which yield model results that “best fit” the data according to an error criteria. Calibration is typically performed as part of a larger set of code verification and validation activities. The context for calibration must be carefully considered: how will the calibrated code be used, how representative is the experimental data of the context in which the code will be used, how much experimental data is available, how accurate and relevant is the experimental data? In some cases, the experimental data may not be sufficient to constrain the parameters. In other cases, different data sets may indicate different optimal values for the parameters, and using all of the data sets may result in parameter value tradeoffs. Understanding the experimental configurations and their design is essential for understanding how to weight and combine experimental data properly in calibration.

2.1. Calibration Algorithms

Typically, calibration problems can be posed as nonlinear regression problems. Nonlinear regression extends linear regression for use with a much larger and more general class of functions [8]. The goal of nonlinear regression is to find the optimal values of θ to minimize the error sum of squares function $S(\theta)$, also referred to as SSE:

$$S(\theta) = \sum_{i=1}^n [f(\theta) - y_i]^2 = \sum_{i=1}^n [r_i(\theta)]^2. \quad (1)$$

Where f is the nonlinear model, y is the observed response, and θ is a vector of parameters.

Nonlinear regression requires an optimization algorithm to find the least squares estimator $\hat{\theta}$ of the true minimum θ^* . This is often difficult. Nonlinear least squares optimization algorithms based on Gauss-Newton approaches have been designed to exploit the structure of a sum of the squares objective

function. If $S(\boldsymbol{\theta})$ is differentiated twice, terms of residual $r_i(\boldsymbol{\theta})$, $r_i''(\boldsymbol{\theta})$, and $[r_i'(\boldsymbol{\theta})]^2$ result. By assuming that the residuals $r_i(\boldsymbol{\theta})$ are close to zero near the solution, the Hessian matrix of second derivatives of $S(\boldsymbol{\theta})$ can be approximated using only first derivatives of $r_i(\boldsymbol{\theta})$. As a result, Gauss-Newton algorithms exhibit quadratic convergence rates near the solution for those cases when the Hessian approximation is accurate, i.e. the residuals tend towards zero at the solution. Thus, by exploiting the structure of the problem, the second order convergence characteristics of a full Newton algorithm can be obtained using only first order information from the least squares terms.

We use a variant of the Gauss-Newton algorithm called NL2SOL [9]. The NL2SOL algorithm is a secant-based least-squares algorithm that is q -superlinearly convergent. It adaptively chooses between the Gauss-Newton Hessian approximation and an approximation augmented by a correction term from a secant update. NL2SOL is more robust than many Gauss-Newton based least-squares solvers which experience difficulty when the residuals at the solution are significant. NL2SOL is appropriate for large residual problems, i.e., least-squares problems for which the residuals do not tend towards zero at the solution.

Note that the Gauss-Newton and NL2SOL formulations typically require the user to explicitly formulate each term in the least squares (e.g., n terms for n data points) along with the gradients for each term. This may be very expensive for computationally intensive evaluations of f . The number of necessary calculations also will increase as the number of parameters increases. Additionally, the approximation of gradients in the presence of errors in the problem is problematic. Often, the gradient approximation has larger errors than the objective function approximation: the accuracy of the gradient is a critical element in these optimization approaches.

In addition to gradient-based methods, we consider a derivative-free, global optimization method called DIRECT (DIviding RECTangles) [10]. The DIRECT optimization algorithm is a global optimization method that balances local search in promising regions of the design space with global search in unexplored regions. DIRECT adaptively subdivides the space of feasible design points so as to guarantee that iterates are generated in the neighborhood of a global minimum in finitely many iterations. In a global method, we simply pass the entire SSE term to the optimizer as one objective: it is not necessary to identify the residuals separately, only their sum-squared-error total.

$$\begin{aligned} & \underset{\boldsymbol{\theta}}{\text{minimize}} && SSE = S(\boldsymbol{\theta}) \\ & \text{subject to bound constraints:} && \theta_{j_{lower}} \leq \theta_j \leq \theta_{j_{upper}}, \quad j = 1, \dots, m. \end{aligned} \tag{2}$$

There is a tradeoff between derivative-free, global optimization methods, and local optimization methods that incorporate derivatives. Global methods are usually better at finding an overall minimum or set of minima, and do not require the calculation of gradients which can be expensive, especially for high-dimensional problems. However, global methods often require more function evaluations. Local methods usually converge fairly quickly and require fewer function evaluations, but they are very dependent on the choice of initial starting point. Local methods tend to find the optimum that is in the vicinity of the starting point; if there are multiple minima, they will stop after finding the closest one and not do a global exploration of the space. In practice, least-squares solvers such as Gauss-Newton will tend to be significantly more efficient than general-purpose optimization algorithms when the Hessian approximation is a good one, e.g., when the residuals tend towards zero at the solution. Specifically, they can exhibit the quadratic convergence rates of full Newton methods, even though only first-order information is used. However, Gauss-Newton-based least-squares solvers may experience difficulty when the residuals at the solution are significant. In Section 4, we present results from both the NL2SOL algorithm and the DIRECT algorithm.

2.2. DAKOTA Software

DAKOTA allows a user to design computer experiments, run parameter studies, perform uncertainty quantification, and calibrate parameters governing their simulation model. A primary goal for DAKOTA is to provide scientists and engineers with a systematic and rapid means to obtain improved or optimal designs or understand sensitivity or uncertainty using simulation-based models. These capabilities generally lead to improved designs and better understanding of system performance. In addition to providing a practical environment for answering system performance questions, the DAKOTA toolkit provides an extensible platform for the research and rapid prototyping of customized methods and strategies [12].

The DAKOTA toolkit provides a flexible, extensible interface between a simulation code and a variety of iterative methods and strategies. While DAKOTA was originally conceived as an easy-to-use interface between simulation codes and optimization algorithms, recent versions have been expanded to interface with other types of iterative analysis methods such as uncertainty quantification with nondeterministic propagation methods, parameter estimation with nonlinear least squares solution methods, and sensitivity/variance analysis with general-purpose design of experiments and parameter study capabilities. These capabilities may be used on their own or as building blocks within more sophisticated strategies such as hybrid optimization, surrogate-based optimization, or optimization under uncertainty.

Thus, one of the primary advantages that DAKOTA has to offer is access to a broad range of iterative capabilities through a single, relatively simple interface between DAKOTA and a simulator. In this context, we interfaced DAKOTA to BISON. To perform different types of analyses, it is only necessary to change a few commands in the DAKOTA input and start a new analysis. The need to learn a completely different style of command syntax and the need to construct a new interface each time you want to use a new algorithm are eliminated. For the work presented below, we were able to develop one interface between DAKOTA and BISON, and swap out a few lines in the DAKOTA input file to run the derivative free DIRECT optimization after we ran the NP2SOL optimization.

3. MODEL AND EXPERIMENT BACKGROUND

3.1. Fuel fracture in BISON

In ceramic fuel such as UO_2 , a significant temperature gradient develops from the fuel center to the radial edge. This gradient appears during the initial rise to power, inducing stresses of sufficient magnitude to fracture the fuel. The cracks increase the effective fuel volume and decrease the pellet-clad gap width. Because the gas-filled gap represents a large thermal resistance, fuel fracture models have a strong effect on fuel temperature. Two approaches are available in BISON to account for pellet fracture: a simple empirical fuel relocation model and a smeared cracking model.

The relocation model is taken from the ESCORE code [6] and given by:

$$\left(\frac{\Delta D}{D_o}\right)_{REL} = 0.80Q_r\left(\frac{G_t}{D_o}\right)(0.005Bu^{0.3} - 0.20D_o + 0.3) \quad (3)$$

where ΔD is the change in pellet diameter due to relocation, D_o is the as-fabricated cold pellet diameter (inches), G_t is the as-fabricated cold diametral gap (inches), and Bu is the pellet average fuel burnup

(MWd/MTU). Q_r is a dimensionless function of the pellet average linear heating rate q' given by:

$$\begin{aligned} Q_r &= 0 \text{ for } q' \leq 6 \text{ kW/ft} \\ Q_r &= (q' - 6)^{1/3} \text{ for } 6 \text{ kW/ft} < q' \leq 14 \text{ kW/ft} \\ Q_r &= (q' - 10)/2 \text{ for } q' > 14 \text{ kW/ft.} \end{aligned}$$

Note that this model is completely empirical and not dimensionally consistent. As originally reported [6], relocation strains do not activate until a threshold power of 6 kW/ft (19.7 kW/m); as noted above, there is currently not consensus on the optimal value for this threshold.

The smeared cracking model is more mechanistic following the approach outlined in [11], where cracking is simulated by adjusting the elastic constants at material points. This is in contrast to a discrete cracking model, where topographic changes are made to the finite element mesh. When the smeared cracking model is active, principal stresses are compared to a critical stress. If the material stress exceeds the critical stress, the material point is considered cracked in that direction, and the stress is reduced to zero. From that point on, the material point will have no strength unless the strain becomes compressive.

3.2. Halden Experiments and BISON Fuel Rod Model

The experiments referred to as IFA-431 and IFA-432 were heavily instrumented assemblies irradiated in the Halden Boiling Water Reactor (HBWR) in Norway. We used data from three instrumented rods in IFA-431 and three instrumented rods in IFA-432. The tests provided a large amount of well-characterized data under realistic LWR conditions, and have been used extensively for assessing and improving fuel rod performance calculations [13]. Measurements included fuel centerline temperature histories from thermocouples located in the top and bottom end of the fuel column, as shown schematically in Fig. 1(a). All test rods contained fresh high density (95% TD) sintered UO₂ in Zircaloy 2 cladding. The reactor was operated at typical BWR conditions. Details concerning rod geometry and materials, power history and axial power profile, and reactor operating conditions, are given in references [14] and [15]. Although measurements were taken through an extended fuel life, the focus here is on beginning of fuel life, before more complex behavior associated with irradiation and high burnup occurs.

The test rods were analyzed assuming 2D axisymmetry. The fuel column was modeled as a single cylinder (smeared pellets), with a top and bottom hole along the symmetry axis to accommodate the thermocouples. The clad was modeled as a simple cylindrical tube with end caps and an upper plenum. A typical finite element mesh is shown in Fig. 1(b).

3.3. Fracture model comparison

As a preliminary study attention was focused on IFA-432 Rod 1, and three simulations were run to compare different approaches to modeling pellet fracture. Fuel fracture was simply ignored in a first case, followed by simulations using either the relocation or smeared cracking models. For the smeared cracking analysis, only radial cracking was permitted and a fracture strength of 130 MPa was assumed.

Figure 2 compares BISON predictions to temperature measurements from the upper thermocouple during initial power-up. Ignoring fuel fracture results in an over-prediction of approximately 200 K at the highest power considered, which is not unexpected due to an unrealistically large fuel-clad gap. Using the default

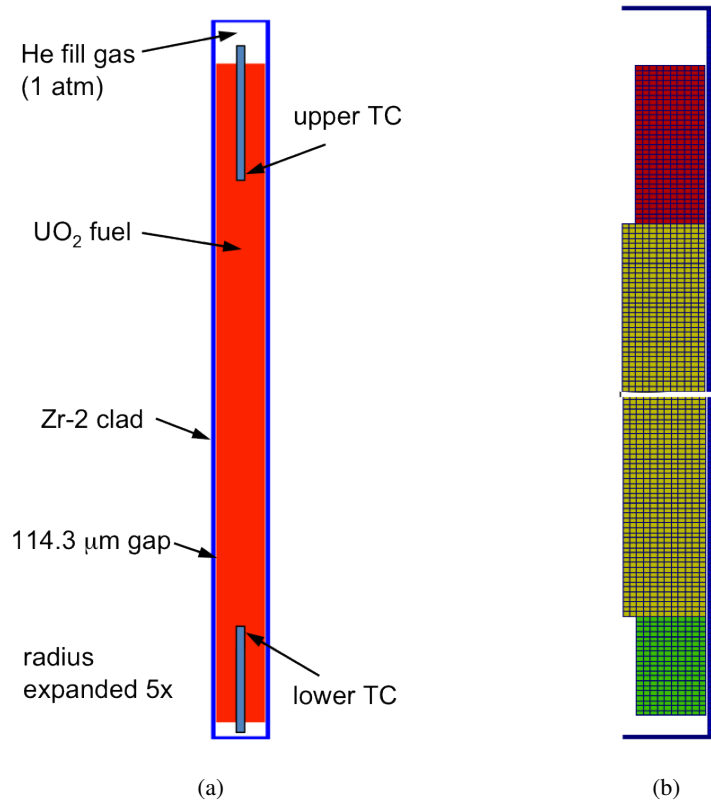


Figure 1. (a) Overview schematic of a Halden IFA fuel rod (aspect ratio scaled 4x) and (b) a typical finite element mesh (aspect ratio scaled 10x). Only the top and bottom regions of the mesh are shown.

relocation model results in a reasonable comparison to experiment. Note in this case the significant change in slope at roughly 20 kW/m, corresponding to relocation activation at the default power threshold of 19.7 kW/m. Interestingly, the smeared cracking model provides a result roughly midway between the other two predictions. This result makes intuitive sense, since the smeared cracking model applied here accounted for only radial cracking and ignored axial and circumferential fracture.

Although nonmechanistic and highly empirical, relocation models are still widely used in fuel performance analyses. Systematic calibration of such models to experimental data is important and the focus of the remainder of this study.

4. RELOCATION CALIBRATION STUDY

4.1. Calibration with a single rod: IFA-432, Rod 1

To optimize the power threshold at which the relocation model is activated, we examined two approaches as described above: the gradient-based nonlinear least squares solver NP2SOL, and the global optimization method DIRECT. Note that the formulation is similar for both models: the objective is to find the value of the relocation activation threshold which minimizes the sum-of-squares error term (e.g. the difference between the BISON results and the Halden thermocouple data). The value of the relocation activation parameter which minimizes the sum-of-squares error (SSE) term will be considered the optimal parameter.

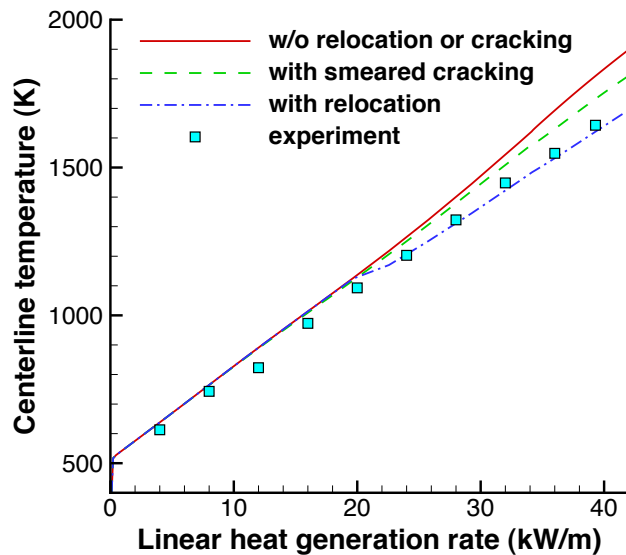


Figure 2. Comparison of IFA-432 Rod 1 upper thermocouple temperature prediction using different BISON fuel fracture models

In most calibration problems, it is necessary to explore the optimization space so that one has an idea if there are many values of the calibration parameters which yield similar optimal values of SSE (e.g. multiple local optima) or if there is one overall optimum. The bounds we set on the relocation activation power were from 0 to 20000 W/m, or from 0 to 6.1 kW/ft.

For the first rod in the IFA-432 experiment, the Halden data was taken in 15-minute increments to generate 32 data points each for the lower and upper thermocouple, for a total of 64 data points. We set up the postprocessor in BISON to print out the temperature at the corresponding times as the Halden data set. We also set up the postprocessor to output the temperatures at both the upper and lower thermocouple locations. Thus, we had a total of 32 upper thermocouple observations and 32 upper thermocouple temperature predictions from BISON to compare, and the same number of observations and BISON predictions for the lower thermocouple, for a total of 64 residual terms in the SSE calculation.

First we describe the results from DIRECT. We ran DIRECT a few times, with different limits on the number of function evaluations. The first time we ran DIRECT, we got an optimal value of SSE = 117866, at a relocation power threshold of 12642.9 W/m. This took 105 function evaluations to run. The longest run we did in DIRECT took 171 function evaluations, but the optimal result was the same. We plot the SSE as a function of the relocation power threshold in Figure 3.

Figure 3 shows a few interesting characteristics: overall, the SSE has a quadratic nature. Gradient-based methods work extremely well on these problems, but there are these small “bumps” and discontinuities in the SSE objective function near the optimum which will cause problems for gradient-based methods. For example, if we start NL2SOL at 10,000 W/m, it goes to a local optimum of 11206.9W/m, for a SSE value of 118071.5. Note that this is not as good as the DIRECT SSE value of 117866, but it is close, and it only

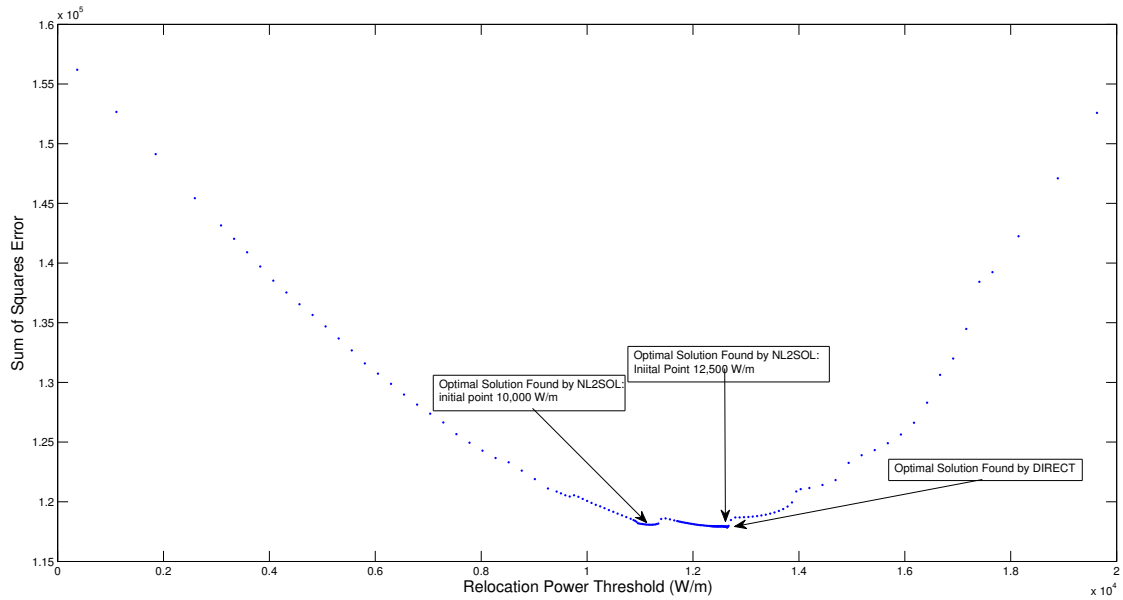


Figure 3. SSE as a function of Relocation Activation Power Threshold, with various Optimization Results

took NL2SOL 13 function evaluations to get to this answer. If we start NL2SOL at 12,500 W/m, the answer converges even sooner: NL2SOL only takes five function evaluations to produce an optimal solution of 117938.6 at a relocation activation value of 12533.24 W/m. Again, this is not quite as good as DIRECT but only required three function evaluations plus two additional ones for derivative calculations, vs. the 105 function evaluations required for DIRECT.

This Halden experiment was run once for IFA-432 Rod 1, so we have one set of data to which we compare the BISON results. Although we have the data at 32 time points and 2 locations, we essentially have one data point (e.g. if we run BISON once, we get the entire set of results to compare to the observational data). Thus, this problem is really a single input, single observation problem. When we change the value of the relocation parameter in the NL2SOL gradient-based method by a small increment, we get ALL of the values of the derivatives of the residuals. That is, in one step in the input parameter space, we are able to obtain the derivatives of the 64 residuals. This is what makes the problem so efficient and why we can obtain a local minimum in five function evaluations when starting from a good initial point. If we were to have to run a separate BISON model to obtain the values of the residuals at each of the 64 data points, that would involve much more computation. Similarly, if we had five data sets of 64 points for the same rod, we would need to perform more postprocessing to obtain the residuals for all of these data sets.

4.2. Calibration for multiple rods: IFA-432, Rods 1, 2, and 3

In this section, we focus on a comparison of the optimal values of the relocation activation threshold for the three rods in the Halden IFA-432 experiment. When we calibrate the relocation activation threshold separately for each rod, we see the differences shown in Figure 4. Rod 1 (which has an optimal relocation threshold value of about 12,640 W/m) is similar to Rod 2, which has an optimal value near 14,000 W/m. Note that Rod 2 only had a lower TC reading to calibrate against: that is why the whole curve is shifted

down (lower sum-square-error) but it has a similar shape to Rod 1. However, the error curve for Rod 3 is different: the optimal value is at zero. We can see the differences in the individual rod predictions as shown in Figure 5. The BISON model tends to overpredict the temperature for the lower thermocouple but underpredict the temperature for the upper thermocouple for Rod 1 on the left side of this figure. However, the BISON model overpredicts the temperatures for both thermocouples for Rod 3, especially the first one. This drives the relocation activation threshold to be turned on at zero.

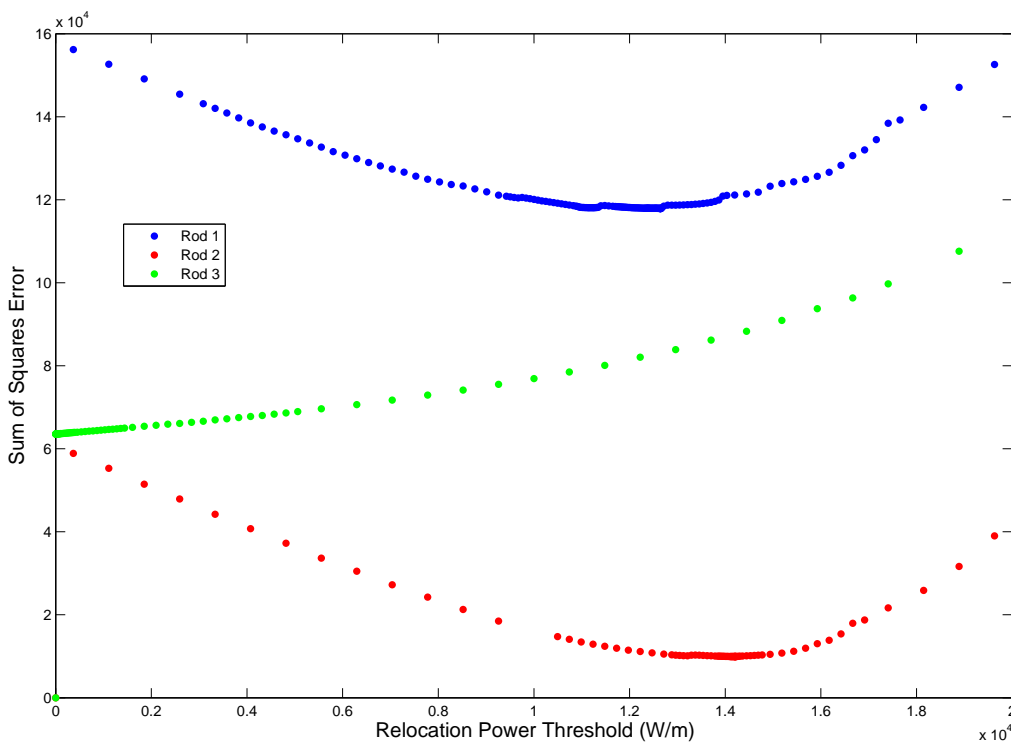


Figure 4. SSE as a function of Relocation Activation Power Threshold for the three Halden IFA-432 Rods

4.3. Calibration with multiple rods: IFA-431 and IFA-432, Rods 1, 2, and 3 each

In this section, we address the aggregated or simultaneous optimization problem: we wish to find the value of the relocation activation threshold that optimizes the error with respect to all of the data we have for the IFA-431 and IFA-432 experiments, which involves 6 rods in total. We formulated this as a global optimization problem. For each value of the relocation activation that was determined by the DIRECT algorithm in DAKOTA, we launch six BISON runs, one for each rod. We wrote a script that aggregated the sum of squares errors from all six rods, including the upper and lower thermocouple errors for each rod. This error as well as the individual errors per rod were returned to DAKOTA. The optimization results are shown in Figure 6.

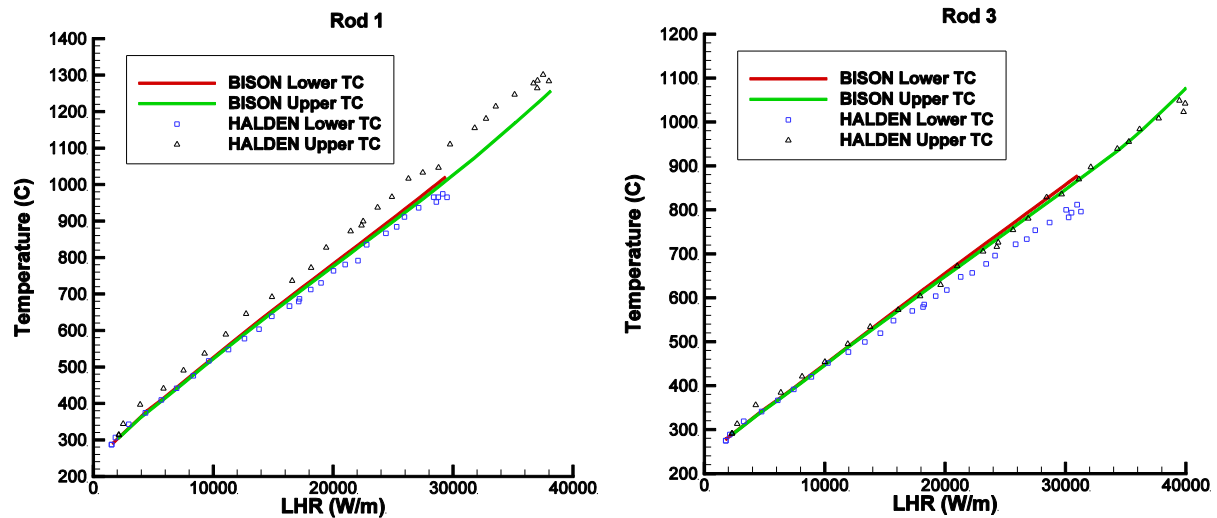


Figure 5. Comparison of BISON temperature predictions for IFA-432 Rods 1 and 3.

In this figure, the total error is shown in black. Rod 1 is shown in blue (solid blue for IFA-432 and open circle for IFA-431), Rod 2 is shown in red, and Rod 3 is shown in green. Note the optimal value for the relocation activation threshold for all three of the IFA-431 rods is zero. This result, along with the result that the optimal value for the IFA-432 Rod 3 was zero, drives the behavior of the aggregated calibration. It is interesting to note, however, that the the sum of squared error is relatively flat between 0 and 5000 W/m. The SSE has a value of approximately 620000 at a relocation activation near zero but approximately 660000 near a relocation activation threshold of 5000 W/m. Given the magnitude of these errors, this is a relatively small difference of six percent. Our interpretation is that any value between zero and 5000 W/m seems to give fairly consistent and robust results. Note that if one weighted either the individual measurements differently (e.g. weighted one or more of the rods more heavily than the others, or one of the thermocouple readings more than the other), the optimal value based on the aggregate data would be different.

Although based on a limited data set (6 rods, 11 measurements) this study recommends a power activation threshold (0-5 kW/m) much lower than the 19.7 kW/m value recommended previously [6]. However, other evidence suggests a lower threshold value may be appropriate. For example, an early experimental study of nuclear fuel cracking concluded that pellets simultaneously crack and increase their diameters when the rod power reaches approximately 6 kW/m [16]. Additionally, multiple simplistic relocation models activate on the first time step, corresponding to the first rise to any power [17].

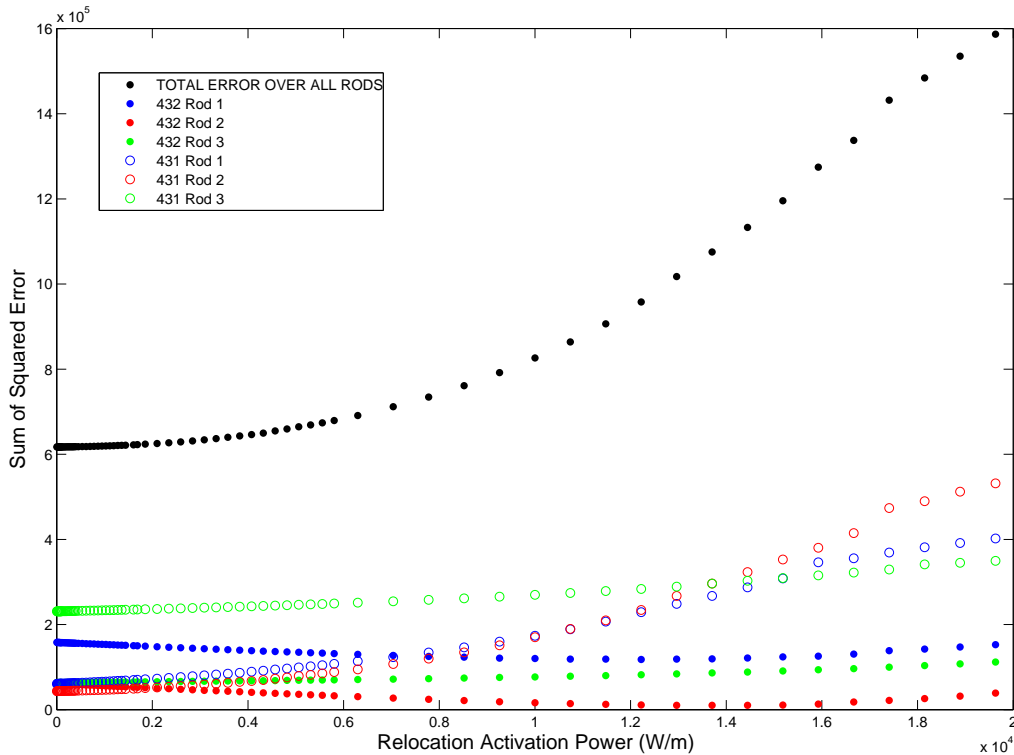


Figure 6. SSE as a function of Relocation Activation Power Threshold, with various Optimization Results

5. SUMMARY

In this paper, we presented results for the calibration of the relocation activation parameter governing the BISON fuel relocation model. We compared local and global optimization methods, and demonstrated the advantages of each. We performed calibration of the relocation activation parameter to individual rods, and showed that the optimal value does vary across rods. We also demonstrated an aggregated calibration, where we used observations from six rods in the parameter estimation. Future work will include the incorporation of other variables and additional observations, as well as uncertainty from other sources (e.g. other models, systematic bias, etc.)

ACKNOWLEDGEMENTS

This work was funded by the Nuclear Energy Advanced Modeling and Simulation (NEAMS) Program under the Advanced Modeling and Simulation Office (AMSO) in the Nuclear Energy Office in the U.S. Department of Energy. The authors acknowledge the help of the MOOSE development team and Jason Hales. The authors also acknowledge the support of the Program Manager of the Fuels Product Line, Steven Hayes (INL), and the NEAMS National Technical Director, Keith Bradley (ANL).

REFERENCES

- [1] R.L. Williamson, J.D. Hales, S.R. Novascone, M.R. Tonks, D.R. Gaston, C.J. Permann, D. Andrs and R.C. Martineau, "Multidimensional multiphysics simulation of nuclear fuel behavior," *J. Nuc. Mat.*, **423**, pp. 149-163, (2012). Available at: <http://dx.doi.org/10.1016/j.jnucmat.2012.01.012>.
- [2] D. Gaston, C. Newman, G. Hansen and D. Lebrun-Grandi, "MOOSE: A parallel computational framework for coupled systems of nonlinear equations," *Nuc. Eng. Des.*, **239**, pp. 1768-1778, (2009). Available at: <http://dx.doi.org/10.1016/j.nucengdes.2009.05.021>.
- [3] D. M. Perez, R. L. Williamson, S. R. Novascone, T. K. Larson, J. D. Hales, B.W. Spencer, and G. Pastore, "An Evaluation of the Nuclear Fuel Performance Code BISON." *International Conference on Mathematics and Computational Methods Applied to Nuclear Science and Engineering, 2013*.
- [4] G. A. Berna, C. E. Beyer, K. L. Davis and D. D. Lanning, "FRAPCON-3: A Computer Code for the Calculation of Steady-State, Thermal-Mechanical Behavior of Oxide Fuel Rods for High Burnup," *NUREG/CR-6534 Vol. 2, PNNL-11513* (1997)
- [5] K. Lassmann, "A. Schubert and J. van de Laar, TRANSURANUS Handbook," *Document Number Version 1 Modification 1 (VIMI2003), European Commission Joint Research Centre Institute for Transuranium Elements* (2003).
- [6] Y. Rashid, R. Dunham and R. Montgomery, "Fuel Analysis and Licensing Code: FALCON MOD01," *Electric Power Research Institute Report: EPRI 1011308*, Dec. 2004.
- [7] R. L. Williamson, "Simulation of NGNP Fuel Using the BISON Fuel Performance Code: 2010 Progress Report," *INL/EXT-11-21403* (2011)
- [8] G. A. F. Seber and C. J. Wild, *Nonlinear Regression*, Wiley, New Jersey, USA (2003).
- [9] J. E. Dennis, D. M. Gay, and R. E. Welsch. "ALGORITHM 573: NL2SOL: An adaptive nonlinear least-squares algorithm." *ACM Trans. Math. Software*, **7**, pp. 369-383, (1981).
- [10] J. M. Gablonsky and C. T. Kelley, "A locally-biased form of the DIRECT algorithm," *J. Global Optimization*, **21(1)**, pp. 27-37 (2001).
- [11] Y. R. Rashid, "Mathematical modeling and analysis of fuel rods" *Nuc. Eng. Des.*, **29**, pp. 22-32 (1974).
- [12] B. M. Adams, W. J. Bohnhoff, K. R. Dalbey, J. P. Eddy, M. S. Eldred, P.D. Hough, S. Lefantzi, L. P. Swiler, and D. M. Vigil, D. M. "DAKOTA: A Multilevel Parallel Object-Oriented Framework for Design Optimization, Parameter Estimation, Uncertainty Quantification, and Sensitivity Analysis. Version 5.2 Users Manual," *Sandia Technical Report SAND2010-2183*, updated Nov. 2011.
- [13] NUREG/CR-2567. "Final Data Report for the Instrumented Fuel Assembly (IFA)-432", prepared by E. R. Bradley, M. E. Cunningham and D. D. Lanning. Battelle Pacific Northwest Laboratory, prepared for the Nuclear Regulatory Commission (1982).
- [14] NUREG/CR-4717. "Irradiation History and Final Postirradiation Data for IFA-432", prepared by D. D. Lanning. Battelle Pacific Northwest Laboratory, prepared for the Nuclear Regulatory Commission (1986).
- [15] NUREG/CR-0560. "Data Report for the NRC/PNL Halden Assembly IFA-432." Prepared by C. R. Hann, E. R. Bradley, M. E. Cunningham, D. D. Lanning, R. K. Marshall, and R. E. Williford. Battelle Pacific Northwest Laboratory, prepared for the Nuclear Regulatory Commission (1978).
- [16] M. Oguma, "Cracking and relocation behavior of nuclear fuel pellets during rise to power," *Nuc. Eng. Des.*, **76**, pp. 35-45, (1983).
- [17] K. Lassmann and H. Blank, "Modeling of fuel rod behavior and recent advances of the TRANSURANUS code," *Nuc. Eng. Des.*, **106**, pp. 291-313, (1988).